Journal of Electronic Materials (2022) 51:4978–4985
https://doi.org/10.1007/s11664-022-09730-4

ORIGINAL RESEARCH ARTICLE

Study of Electronic, Optoelectronic and Photonic Properties of NBB Material in Solvent Environments

Emine Tanış[1]

Received: 10 November 2021 / Accepted: 23 May 2022 / Published online: 17 June 2022

Abstract

Here, the effects of dimethyl sulfoxide (DMSO), ethanol and tetrahydrofuran (THF) solvents on the electronic, optoelectronic and photonic properties of *N*-butyl-1*H*-benzimidazole (NBB) organic material were investigated in detail with experimental measurements' suitable. Quantum chemical calculations including absorbance spectrum, HOMO–LUMO, and OPDOS spectrum were performed with the help of density functional theory and compared with experimental results NBB material has a middle-ultraviolet absorbance spectrum in the range of 248–295 nm for the studied solvents and near-ultraviolet emission spectrum at 311 nm in THF solvent. Similarly, the optical bandgap ranged from 4.16 eV to 4.26 eV and is compatible with both the optoelectronic device technology and the HOMO–LUMO energy gap. It was determined that the electrical conductivity of the material is higher than its optical conductivity. From all the results obtained, it can be concluded that NBB material may be a suitable candidate for optoelectronics and photonics technology in all relevant solvents.

Keywords NBB · photonic · optoelectronic · quantum chemical calculations

Introduction

In recent years, there has been a great interest in the search for new materials in the field of organic electronics, such as organic light-emitting diodes, organic field-effect transistors, and organic solar cells.[1–3] In these material studies, benzimidazole, which is an *N*-heterocyclic compound of the π-conjugate class consisting of a combination of benzene and imidazole rings, and its derivatives have been the subject of intense study.[4–8] Benzimidazole and its derivatives are known as electron-transporting materials in organic electronics due to their good electron mobility and injection.[9–13] In addition, compounds containing benzimidazole units have high stability and strong electron-accepting capacity.[14,15] Shannon et al.[16] determined the capacity of butylbenzimidazole to hold SO_2 and CO_2 gases depending on temperature and alkyl chain length. Üstün et al.[17] reported the structural, electronic and reactivity properties of molybdenum and tungsten carbonyl complexes using the butylbenzimidazole ligand. Jaehyun and colleagues[18] also published a study on the butyl group's high performance as the layer emitting brightness and efficiency in an organic light-emitting diode (OLED) device.

Through new methodologies that enable the determination of solvent action, it has been found that solute–solvent interactions are responsible for significant changes in the chemical and physical properties of matter. Therefore, determining the effect of the solvent is critical to understanding the various properties of the molecules of interest.[19]

There is no study in the literature on the optical, electronic and photonic properties of NBB material. We were motivated to conduct this study because of the unique properties of benzimidazole mentioned above. Therefore, in this study, NBB, a benzimidazole derivative, was investigated in detail experimentally and theoretically in terms of electronic, optical and photonic properties in various solutions.

Experimental Details

NBB and ethanol, dimethyl sulfoxide (DMSO) and tetrahydrofuran (THF) were purchased from Sigma-Aldrich Co. LLC in liquid form with purity of above 97%. The molecular weight of the NBB and empirical formula are 174.24 g/mol

✉ Emine Tanış
eminetanis@ahievran.edu.tr

[1] Department of Electrical Electronics Engineering, Kırşehir Ahi Evran University, 40100 Kirsehir, Turkey

and $C_{11}H_{14}N_2$, respectively. The solutions were prepared in DMSO, THF and ethanol solvents for 2.5 nM concentration.

UV spectra of the NBB solutions were recorded in a range of 200–600 nm using a Evolution 201 UV Vis Spectrophotometer. The fluorescence measurement of the NBB solution for THF solvent was carried out with a Hitachi S-7000 fluorescence spectrophotometer at room temperature.

Quantum Chemical Computations

The calculations of the NBB were performed using the Gaussian 09,[20] GaussView 5.0[21] and GaussSum 2.2[22] programs. The TD-DFT/B3LYP function with the 6-311++G(d,p) basis set was used for electronic and optical calculations. The TD-DFT method is known to be one of the most reliable methods for calculating the electronic structure of molecules and complex oxide materials.[23–29] The optimized structure used in quantum chemical calculations is given in Fig. 1. After optimization, electronic calculations were performed for all solvents to compare with the experimental absorbance values.

Results and Discussion

The Absorption and Fluorescence Characteristics of the NBB Solutions

The experimental absorbance results of the NBB molecule depending upon the solvents (DMSO, ethanol and THF) is shown in Fig. 2. The absorbance spectrum of NBB was observed at around 276 nm (4.49 eV) in DMSO, representing the π-π* transition. While NBB peaked at 291 nm (4.26 eV) in ethanol solvent, two absorption peaks were observed in THF solvent at 248 nm (4.50 eV) and 295 nm (4.20 eV), one of which was slightly lower than the other. It is evident from these results that NBB has maximum absorbance peaks in the middle-UV region for all solvents. When compared with the results of poly(methyl methacrylate) (PMMA) and cadmium sulfide (CdS) nanocomposites,[30–32] which are suitable for OLED applications and have an absorption bandgap in the range of 190–330 nm, it can be concluded that NBB may also be a suitable candidate for OLED applications.

Figure 3 shows the correlation bars for experimental and theoretical absorbance results. In Fig. 3 it is seen that the agreement between the two methods is greatest in THF solvent, and the highest error is obtained in ethanol solution.

The fluorescence spectrum, which determines the fluorescence characteristics of the NBB molecule, was measured in THF solution and is presented in Fig. 4. The NBB molecule emits light at 311 nm (or 3.99 eV), while it absorbs light energy at 248 nm (4.50 eV) and 295 nm (4.20 eV) in THF solution. The results show that NBB is a molecule that absorbs light in the middle-UV region and emits light in the near-UV region.

Theoretical UV calculations are carried out using the TD-DFT/B3LYP/6-311++G(d,p) basis set and polarisable

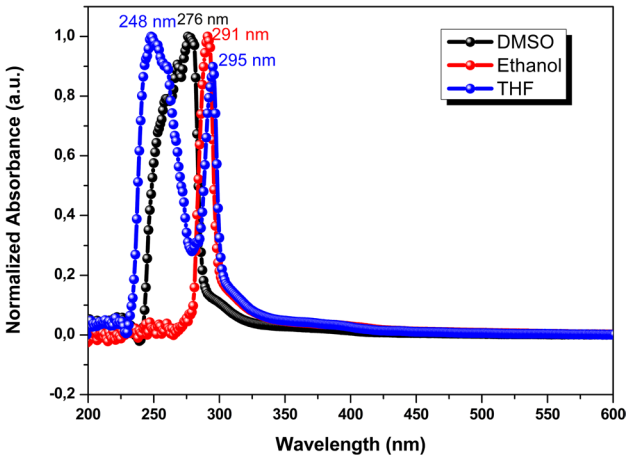

Fig. 2 Experimental absorbance spectra of NBB for different solvents.

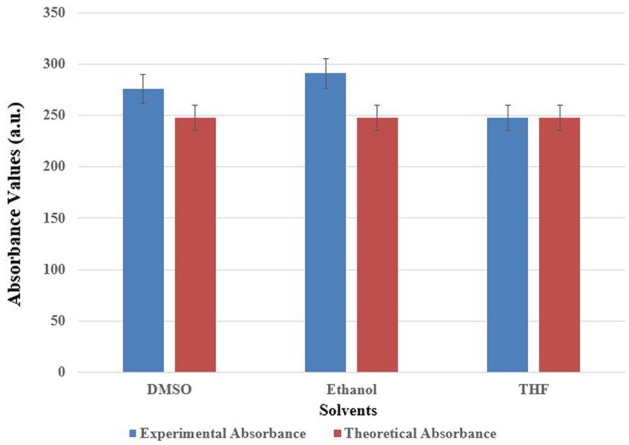

Fig. 3 Correlation bars of calculated and experimental absorbance results.

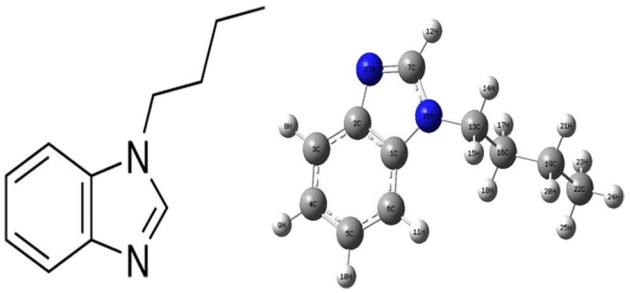

Fig. 1 2D and theoretical optimized geometric structures of *N*-butyl-1*H*-benzimidazole (NBB).

continuum model (PCM) within self-consistent reaction field (SCRF) theory[33] and presented in Fig. 5. Maximum absorbance is 248 nm (4.50 eV) for all solvents, and it is clearly seen from the experimental measurements that this is in perfect agreement with the results in the THF solvent, while it remains at a lower wavelength for other solvents. In addition, the solvent effect is not seen from the results of the theoretical calculations.

Frontier Molecular Orbital (FMO) Analysis

The frontier molecular orbitals, namely highest occupied molecular orbital (HOMO) and lowest unoccupied molecular orbital (LUMO), and the energy difference between these orbitals are important in terms of electronic and optical properties.[34] Figure 6 shows the contour plots of the HOMO and LUMO and the energy values of these orbitals for the NBB. It can be seen that the butyl group partially contributes to the HOMO orbitals, but does not contribute to the LUMO orbitals. HOMO and LUMO energies of the NBB were found to be −9.22 eV and −5.22 eV, respectively. The difference between the HOMO and LUMO energy levels is called the electronic bandgap, which was calculated as 4.0 eV. It is seen that this obtained bandgap value is quite compatible with the electronic bandgap results for the phenyl pyridoindole (Ph-Cb1) molecule, which was found suitable for OLED material design in a previous study.[35]

Also, overlap population density of states (OPDOS) analysis was performed for the NBB molecule to support the boundary molecular orbital diagrams and identify the donor–acceptor moieties and is shown in Fig. 7. For this, the GaussSum 2.2 program[22] was used, and molecular orbital information was combined with unit height and full-width Gaussian curves at half maximum (FWHM) of 0.3 eV. Zero, negative and positive values on the OPDOS spectrum represent non-bonding, anti-bonding and bonding states, respectively. Supporting the results in Fig. 6, it is clearly seen in the OPDOS spectrum that the benzene and imidazole rings contribute the most to the bond orbitals.

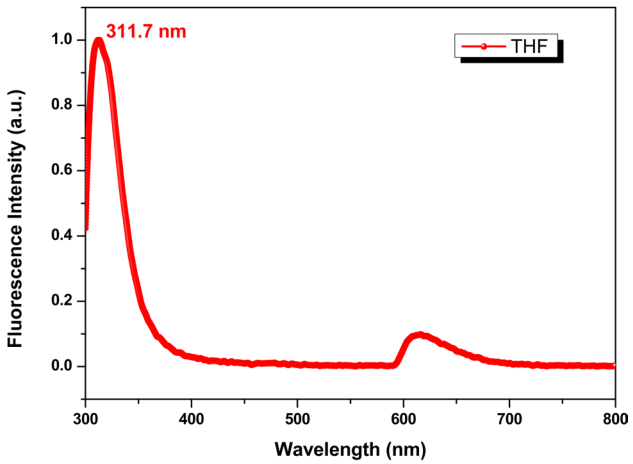

Fig. 4 Experimental fluorescence spectra of NBB for THF solvent.

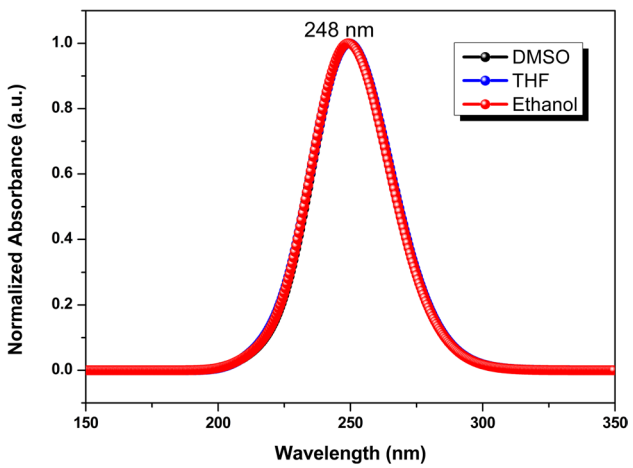

Fig. 5 Theoretical absorbance spectra of NBB for different solvents.

The Bandgap Energy and Refractive Index

The optical bandgap is an important optical parameter that controls the nature of the electroluminescence signal in OLEDs.[34] It can be calculated with the help of the Tauc relation[36] used in the literature[37,38]

$$(\alpha h\nu) = A\left(h\nu - E_g\right)^n \quad (1)$$

where α is the absorption coefficient, A is a constant, $h\nu$ is photon energy, E_g is the optical energy gap, and n is a parameter which measures the types of bandgap. For NBB, the type of bandgap[39] is the direct allowed bandgap (E_g). For this, we plotted the $(\alpha h\nu)^2$ plot versus E of the NBB for DMSO, ethanol and THF solvents, as seen in Fig. 8. We calculated the E_g values from the linear regions of Fig. 8, and the E_g values obtained for the NBB are given in Table I. It can be seen that the E_g value of NBB was approximately 4.20 eV for THF, and approximately 4.16 eV and 4.26 eV for ethanol and DMSO, respectively. These results seem to

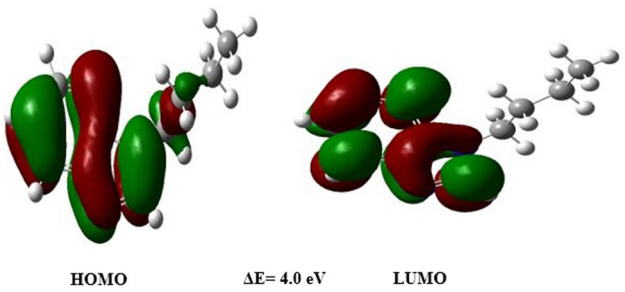

Fig. 6 Frontier molecular orbitals of NBB in gas phase.

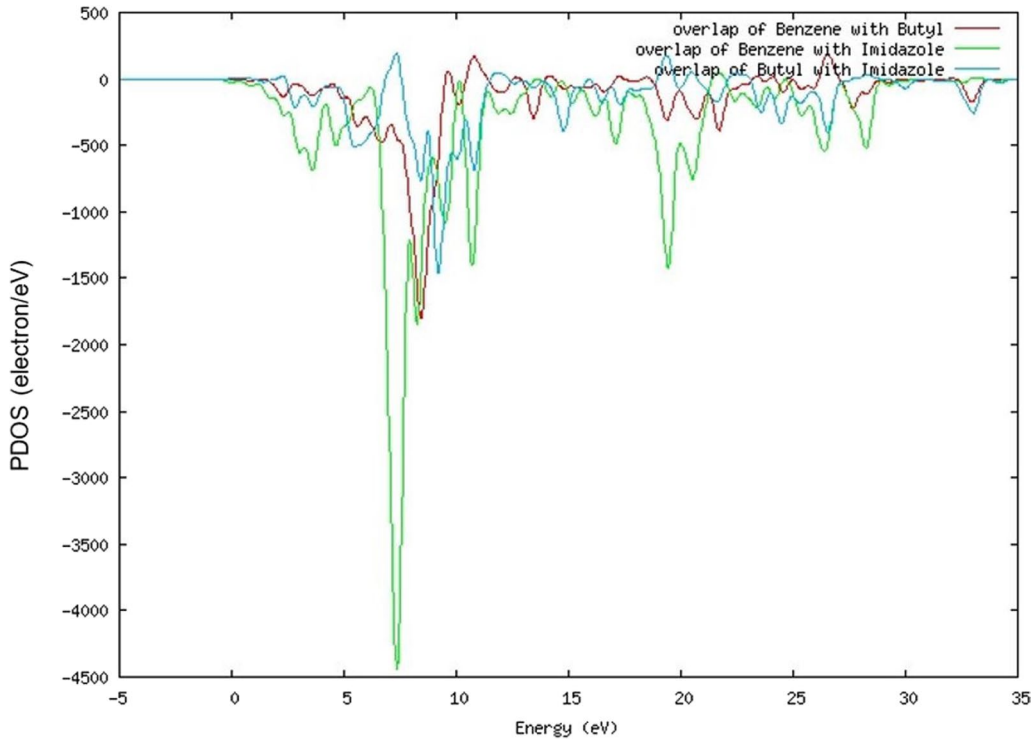

Fig. 7 Partial electronic density of states (PDOS) diagram of NBB.

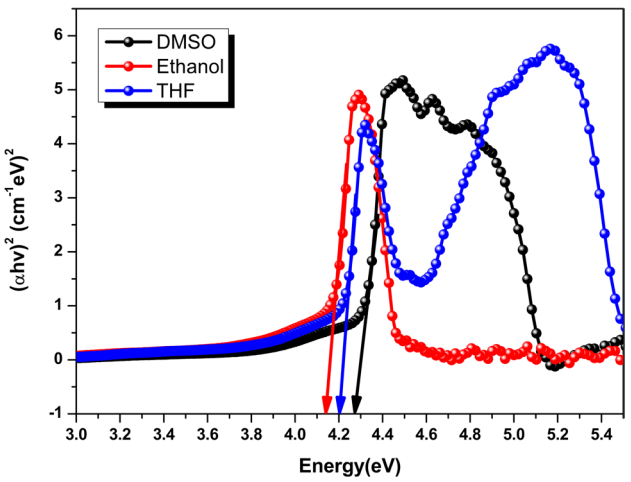

Fig. 8 ($\alpha h\vartheta$)2 curves vs. photon energy (E) of the NBB for different solvents.

Table I The E_g values of the NBB for different solvents

Solvents	E_g (eV)
DMSO	4.26
Ethanol	4.16
THF	4.20

be quite compatible with the energy difference of 4.0 eV between the HOMO–LUMO orbitals. In a previously published study,[40] the optical bandgap of poly(methyl methacrylate) (PMMA) material, which has remarkable electronic and optical properties, was found to be 4.15 eV. This result is very close to the optical bandgap of NBB.

The optical refractive index (n) is an important value for optoelectronics, as it shows how the frequencies and wavelengths of light change as it passes through a transparent material. The experimental n values can be determined by[41]

$$n = \left\{ \left[\frac{4R}{(R-1)^2} - k^2 \right]^{1/2} - \frac{R+1}{R-1} \right\} \tag{2}$$

and are given in Table II. The experimental refractive index values were calculated for all solvents using the experimental optical bandgap. As can be seen from the table, the lowest experimental refractive index is 2.01 in ethanol solvent and the highest is 2.09 in THF solvent. The semi-experimental refractive indices obtained using equations of Moss, Ravindra, Hervé–Vandamme, Reddy and Kumar-Singh[34,42] are presented in Table II. Except for the Hervé–Vandamme results, the results are in good agreement with the experimental ones. When the experimental refractive index values we obtained are compared with PMMA/TiO2,[43–45] a metal

Table II The experimental (Exp.) refractive index (n) parameters and Moss (M), Ravindra (Ra), Hervé–Vandamme (H–V), Reddy (Re) and Kumar-Singh (K–S) relation results of the NBB for different solvents

Solvents	Exp.	Ra	H–V	M	Re	K–S
DMSO	2.03	2.52	3.07	2.48	2.90	2.50
Ethanol	2.01	2.66	3.28	2.54	2.99	2.57
THF	2.09	2.60	3.18	2.51	2.95	2.57

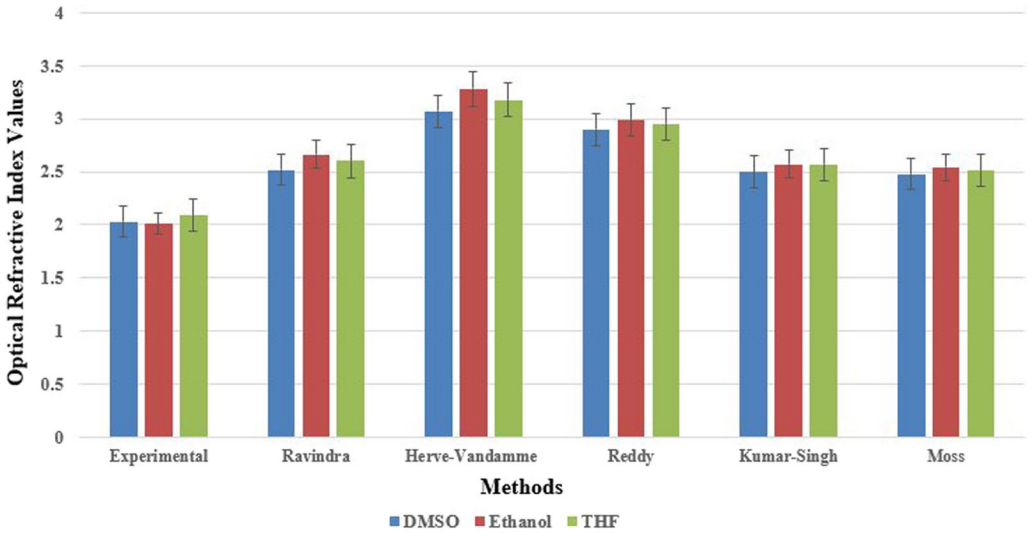

Fig. 9 Correlation bars of experimental and semi-experimental refractive indices results.

oxide nanomaterial, it is seen that NBB is a very suitable candidate for applications such as OLEDs and solar cells.

Figure 9 shows the correlation bars for experimental and semi-experimental refractive index results. In Fig. 8, it is seen that the results closest to the experimental values were obtained in Moss, Kumar-Singh and Ravindra, and the error amount is mostly with the Hervé–Vandamme results.

Figure 10 shows the experimental refractive index (a) and experimental reflectivity (b) as a function of wavelength. Maximum peaks in Fig. 10a are observed at 285 nm, 300 nm and 274 nm for DMSO, ethanol and THF solvents, respectively. The maximum peaks correspond to the approximate optical bandgap value of the sample in the respective solvent. For all solvents, the refractive index values decrease rapidly after the optical bandgap values.

In Fig. 10b, the reflectivity peaks of NBB in DMSO, ethanol and THF solvents are observed at 285 nm, 289 nm and 286 nm, respectively. It is seen that HNMB reflects about 20% of the incident light for all solvents at these wavelengths. After these wavelengths, both refractive index and reflectivity decrease. In addition, it is understood from Fig. 10b that the reflectivity of HNMB increases from 1% to 20% in the range of 274–300 nm in all solvents, This result shows that the sample will mostly absorb the incident light, that is, the absorption property of NBB is good.

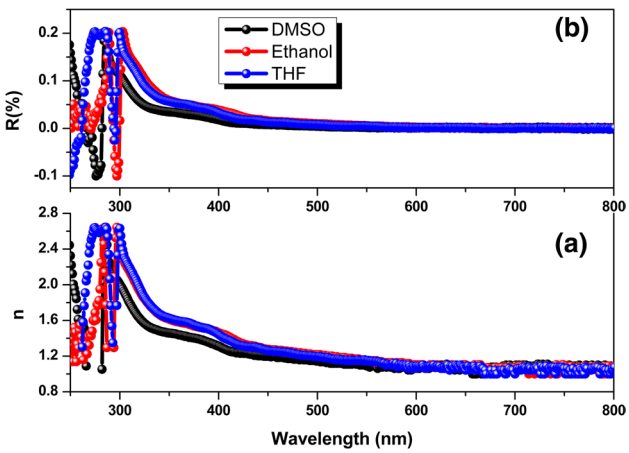

Fig. 10 (a) Reflectivity and (b) refractive index of NBB for different solvents.

Electrical and Optical Conductance

Electrical and optical conductivity are important parameters that determine the optical and photonic properties of high-tech devices.[46–48] They can be calculated with the following equations:

$$\sigma_{optical} = (\alpha nc)/4\pi \tag{3}$$

$$\sigma_{electrical} = \left(\frac{2\lambda}{\alpha}\right).\sigma_{optical} \tag{4}$$

Figure 11a shows the change in optical conductivity in the respective solvents depending on the photon energy. It can be seen from Fig. 11a that when the photon energy is equal to the bandgap of NBB, there is a sudden increase in optical conductivity. The maximum optical conductivity values are around 7.5×10^7 S/m at peaks for all solvents. From this result, it is seen that the optical conductivity does not change according to the solvent. The energy-dependent change in electrical conductivity in the studied solvents is shown in Fig. 11b. Here it is evident that the highest electrical conductivity is at low energies, and its value is around 7×10^{10} S. It is seen that electrical conductivity, like optical conductivity, does not change according to solvents. Also, the electrical conductivity of NBB is much greater than its optical conductivity.

The Photonic Properties

The properties of optoelectronic materials such as the angle of incidence ($\varnothing_1$), refraction angle ($\varnothing_2$), and contrast (α_c) are very important. $\varnothing_1$, $\varnothing_2$ can be given by[49,50];

$$\varnothing_1 = \tan^{-1}\left(\frac{n_2}{n_1}\right) \tag{5}$$

$$\varnothing_2 = \sin^{-1}\left(\left(\frac{n_1}{n_2}\right)\sin\varnothing_1\right) \tag{6}$$

Figure 12a shows the variation in incidence and refraction angle values in respective solvents as a function of energy. The incidence angle of NBB for all solvents increased from ~ 62° to ~ 70°, as seen in Fig. 12a. The energy dependent changes of $\varnothing_2$ values obtained by using Eq. 6 are shown in Fig. 12b. In contrast to the $\varnothing_1$ variation in Fig. 12a, $\varnothing_2$ appears to have a minimum scattering angle at low energies in all solvents. The refraction angle is decreased from ~ 52° to ~ 45°. Also, the $\varnothing_1$ values of NBB are higher than the $\varnothing_2$ values. In a study in the literature,[34] the incidence and refractive angle values are in the visible region range, as they are here, and are greater than our values.

Contrast, which is an important value for determining the sensitivity of NBB, is calculated by the following formula to show the refractive index of n_1 medium and n_2 in the NBB solvent.[51] The variation in contrast versus energy and

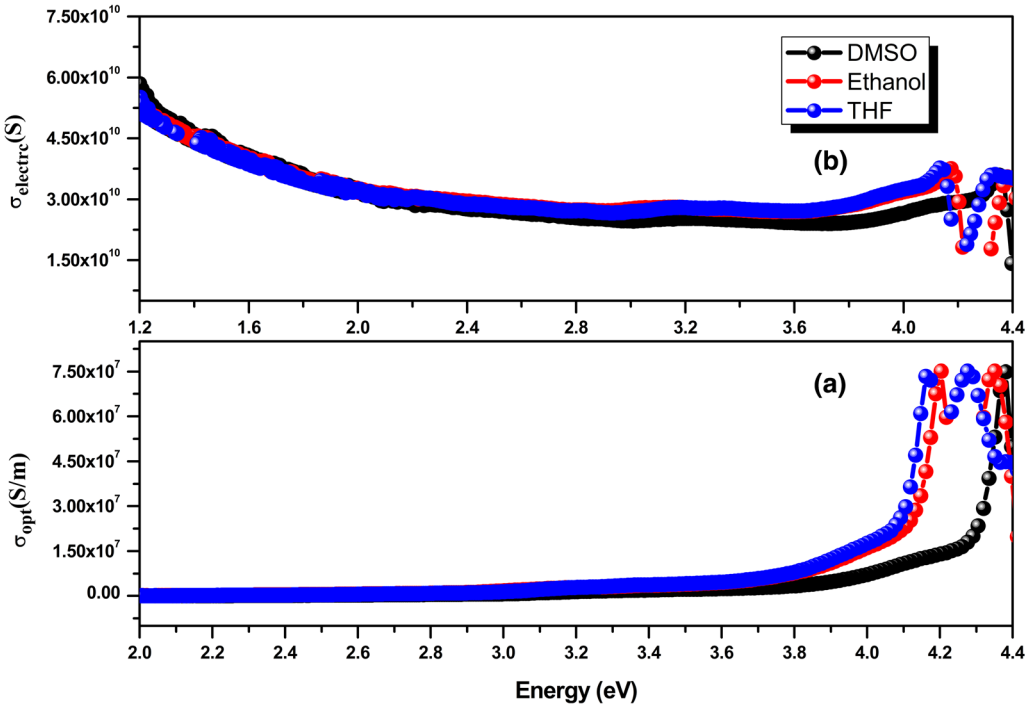

Fig. 11 (a) Optical conductance and (b) electrical conductance values of the NBB for different solvents.

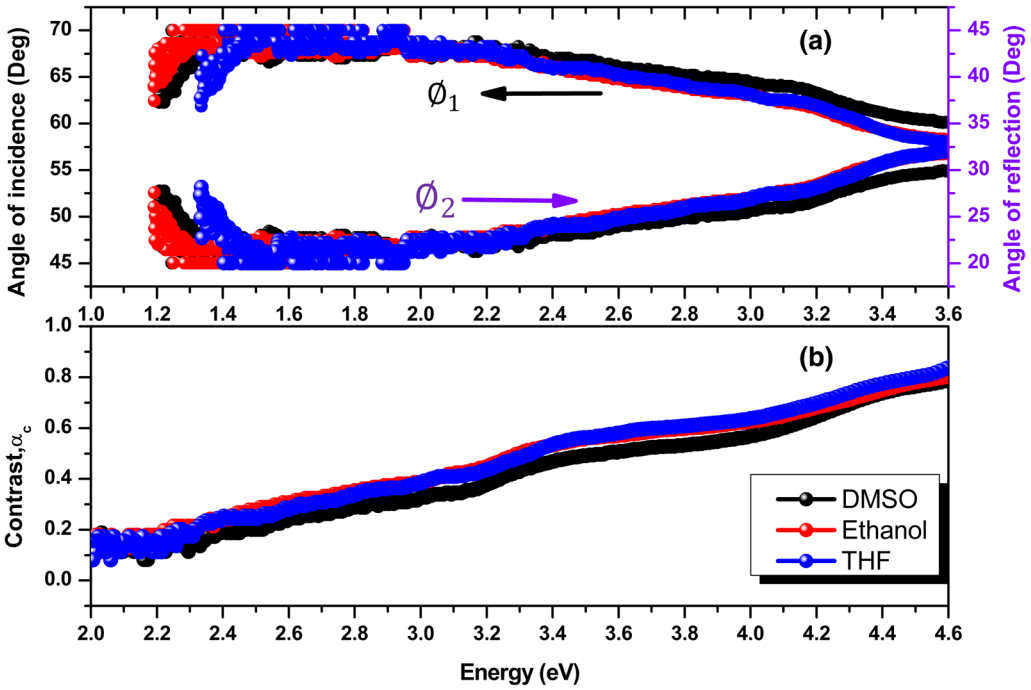

Fig. 12 (a) Angle of incidence and angle of refraction; (b) contrast of NBB for different solvents.

solvents is given in Fig. 10b. It is observed that the contrast increases for all solvents with increasing photon energy.

$$\alpha_c = 1 - \left(\frac{n_1}{n_2}\right)^2 \tag{7}$$

Conclusion

Herein, changes in the electronic, optical and photonic properties of NBB for various solvents were studied in detail. NBB is a molecule that absorbs light in the middle-UV region for all solvents. In addition, for the THF solvent, NBB was found to absorb light in the middle-UV region and emit light in the near-UV region. NBB is a direct-bandgap semiconductor (4.20 eV for THF, approximately 4.16 eV for ethanol and 4.26 eV DMSO). The energy gap value (4.0 eV) between HOMO and LUMO is quite compatible with this measured direct bandgap. The theoretical results are in agreement with the experimental results. The electrical conductivity of NBB is much greater than its optical conductivity. It is understood from the experimental and theoretical results that NBB can be used in photonic and optoelectronic technology with its low refractive index, excellent optical photonic and contrast properties in all studied solvents.

Acknowledgments We are grateful to the research support unit of Kırşehir Ahi Evran University (SAG.A4.20.002), as this work was conducted with their support. The numerical calculations reported in this paper were performed at TUBITAK ULAKBIM, High Performance and Grid Computing Center (TRUBA resources). The author thanks TUBITAK ULAKBİM, High Performance and Network Computing Center for the numerical calculations used in this article.

Conflict of interest The author declares that they have no conflict of interest.

References

1. J. Xie and Q. Zhang, *J Mater. Chem. A* 4, 7091 (2016).
2. Z. Yang, Z. Mao, Z. Xie, Y. Zhang, S. Liu, J. Zhao, J. Xu, Z. Chi, and M.P. Aldred, *Chem. Soc. Rev.* 46, 915 (2017).
3. W. Wu, Q. Chen, R.A. Caruso, and Y. Cheng, *J. Mater. Chem. A.* 5, 10092 (2017).
4. S.H. Park, J.E. Kwon, S.H. Kim, J. Seo, K. Chung, S.-Y. Park, D.-J. Jang, B. Medina, J. Hierschner, and S.Y. Park, *J. Am. Chem. Soc.* 131, 14043 (2009).
5. J.S. Kim, J. Heo, P. Kang, J.H. Kim, S.O. Jung, and S.K. Kwon, *Macromol. Res.* 17, 91 (2009).
6. S.O. Soon, K.S. Yook, and J.Y. Lee, *J. Ind. Eng. Chem.* 34, 407 (2011).
7. J. Huang, J.-H. Su, X. Li, M.-K. Lam, K.-M. Fung, H.-H. Fan, K.-W. Cheah, C.H. Chen, and H. Tian, *J. Mater. Chem.* 21, 2957 (2011).
8. S.-Y. Chang, G.-T. Lin, Y.-C. Cheng, J.-J. Huang, C.-L. Chang, C.-F. Lin, J.-H. Lee, T.-L. Chiu, and M.-K. Leung, *ACS Appl. Mater. Interf* 10, 42723 (2018).
9. P. Dhagat, H.M. Haverinen, R.J. Kline, Y. Jung, D.A. Fischer, D.M. DeLongchamp, and G.E. Jabbour, *Adv. Funct. Mater.* 19, 2365 (2009).
10. A. Babel and S.A. Jenekhe, *J. Am. Chem. Soc.* 125, 13656 (2003).

11. R.P. Ortiz, H. Herrera, R. Blanco, H. Huang, A. Facchetti, T.J. Marks, Y. Zheng, and J.L. Segura, *J. Am. Chem. Soc.* 132, 8440 (2010).
12. C.-H. Chen, W.-S. Huang, M.-Y. Lai, W.-C. Tsao, J.T. Wu, Y.-H. Lin, T.-H. Ke, L.-Y. Chen, and C.-C. Wu, *Versat Adv Funct Mater.* 19, 2661 (2009).
13. W.-Y. Hung, L.-C. Chi, W.-J. Chen, Y.-M. Chen, S.-H. Chou, and K.-T. Wong, *J. Mater. Chem* 20, 10113 (2010).
14. J. Zhao, J. Wong, J. Gao, G. Li, G. Xing, H. Zhang, T.C. Sum, H. Yang, Y. Zhao, S.L. Akejelleberg, W. Huang, S.C.J. Loo, and Q. Zhang, *RSC Adv.* 34, 17822 (2014).
15. M. Masashi, P.B. César, and P. Anzenbacher Jr, *Org. Lett.* 13, 4882 (2011).
16. S.M. Shannon, S.M. Hindman, O.P. Danielsen, M.J. Tedstone, D.R. Gilmore, and E.J. Bara, *Sci China Chem* 55, 1638 (2012).
17. E. Üstün, S. Demir Düşünceli, and İ Özdemir, *Struct Chem* 30, 769 (2019).
18. L. Jaehyun, S. Kim, J.-H. Kim, and J. Park, *J. Nanosci. Nanotech.* 15, 8285 (2015).
19. Y. Liu, H. Du, G. Wang, X. Gong, L. Wang, and H. Xiao, *Int. J. Quant. Chem.* 111, 1115 (2011).
20. Frisch, M.J., Trucks, G.W., Schlegel, H.B., Scuseria, G.E., Robb, M.A., et al., Gaussian 09, Revision A.2, Gaussian, Inc., Wallingford, CT, 2009.
21. R. Dennington, T. Keith, and J. Millam, *GaussView, Version 5* (Shawnee Mission KS: Semichem Inc., 2009).
22. N.M. O'Boyle, A.L. Tenderholt, and K.M. Langner, *J. Comput. Chem.* 29, 839 (2008).
23. M. Jamal, N. Kamali Sarvestani, A. Yazdani, and A.H. Reshak, *RSC Adv.* 4, 57903 (2014).
24. G.W. Ejuh, F. Tchangnwa Nya, N. Djongyang, and J.M.B. Ndjaka, *Optic Quant Electron* 50, 1 (2018).
25. G.W. Ejuh, F. Tchangnwa Nya, R.A. Yossa Kamsi, and J.M.B. Ndjaka, *Polym Bull.* 75, 537 (2018).
26. G.W. Ejuh, F. Tchangnwa Nya, M.T. Ottou Abe, F.J.M.B. Fankam-Jean-Basptiste, and J.M. Ndjaka, *Optic Quant. Electron.* 49, 382 (2017).
27. L.S. Taura, C.E. Ndikilar, G.W. Ejuh, and A. Muhammad, *Mod Appl Sci* 12, 108 (2018).
28. R.I. Eglitis, J. Purans, and R. Jia, *Crystals* 11, 455 (2021).
29. R.I. Eglitis, J. Purans, A.I. Popov, and R. Jia, *Symmetry* 13, 1920 (2021).
30. R.M. Abozaid, Z. Lazarevic´, I. Radovic´, M. Gili´c, D. Sevi´c, M.S. Rabasovi´c, and V. Radojevic, *Opt. Mater.* 92, 405 (2019).
31. M.B. Mohamed and M.H. Abdel-Kader, *Mater. Chem. Phys.* 241, 122285 (2020). https://doi.org/10.1016/j.matchemphys.2019.122285.
32. P.A. Ajibade and J.Z. Mbese, *Int J. Polym. Sci.* 2014, 1 (2014). https://doi.org/10.1155/2014/752394.
33. J. Tomasi, B. Mennucci, and R. Cammi, *Chem. Rev.* 105, 2999 (2005).
34. E. Tanış, *Optik-Int J Light Electr Optic* 252, 168576 (2022).
35. E. Varathan, D. Vijay, and V. Subramanian, *RSC Adv.* 6, 74769 (2016).
36. J. Tauc, *Amorphous and Liquid Semiconductors* (New York: Plenum Press, 1974).
37. R. Yu, M. Yuan, T. Li, Q. Tu, and J. Wang, *RSC Adv.* 6, 90711 (2016).
38. X. Gao and I.E. Wachs, *J. Phys. Chem. B.* 102, 10842 (1998).
39. S. Georges, P. Zhenhua, and H. Shu, *Semiconduct Semimetal* 97, 81–138 (2017).
40. D. Nayak and R.B. Choudhary, *Opt Mater (Amst)* 91, 470 (2019). https://doi.org/10.1016/j.optmat.2019.03.040.
41. F. Abeles, *Optical Properties of Solids* (London and Amsterdam: North-Holland Publishing Company, 1972).
42. S.K. Tripathy, *Opt. Mater.* 46, 240 (2015).
43. J. Schneider, M. Matsuoka, M. Takeuchi, J. Zhang, Y. Horiuchi, M. Anpo, and D.W. Bahnemann, *Chem. Rev.* 114, 9919 (2014). https://doi.org/10.1021/cr5001892.
44. J. Jin, R. Qi, Y. Su, M. Tong, and J. Zhu, *Iran. Polym. J.* 22, 767 (2013). https://doi.org/10.1007/s13726-013-0175-x.
45. Z. Yang, H. Peng, W. Wang, and T. Liu, *J. Appl. Polym. Sci.* 116, 2658 (2010). https://doi.org/10.1002/app.
46. L.Z. Maulana, Z. Li, E. Uykur, K. Manna, S. Polatkan, C. Felser, M. Dressel, and A.V. Pronin, *Phys. Rev. B* 103, 115206 (2021).
47. M. Haghgoo, R. Ansari, and M.K. Hassanzadeh-Aghdam, *Compos Part B: Eng.* 167, 728 (2019).
48. H. Mousavi, *Opt. Commun.* 285, 3137 (2012).
49. N.M. Grebenikova, K.J. Smirnov, V.V. Artemiev, V.V. Davydov, S.V. Kruzhalov, and I.O.P. Conf, *Series: J Phys: Conf Series* 1038, 012089 (2018). https://doi.org/10.1088/1742-6596/1038/1/012089.
50. S. Adachi, *Optical Constants of Crystalline and Amorphous Semiconductors* (Academic Publishers: Kluwer, 1999).
51. A. Purniawan, G. Pandraud, T.S.Y. Moh, A. Marthen, K.A. Vakalopoulos, P.J. French, and P.M. Sarro, *Sens. Actuat A* 188, 127 (2012).